^{99m}Tc-LHRH in tumor receptor imaging

DAWEI HAO, LINGFEI SUN, XIANG HU and XIAOWEN HAO

Department of Radiotherapy, Xuzhou Central Hospital, Xuzhou, Jiangsu 221009, P.R. China

Received June 20, 2016; Accepted December 13, 2016

DOI: 10.3892/ol.2017.6246

Abstract. Detection of gonadotropin-releasing hormone (GnRH) also known as luteinizing hormone-releasing hormone (LHRH) in the relevant tumor tissue and normal tissues and organs *in vivo* expression was investigated. To examine the method of direct radio labeling of LHRH by ^{99m}Tc with relatively high radiochemical purity and stability, screening the best labeling conditions, to establish a simple and reliable method of preparation of ^{99m}Tc-LHRH was undertaken. The detection of radioisotope-labeled LHRH distribution in mice, LHRH receptor imaging for the study and treatment of cancer basis were evaluated. i) Immunohistochemical staining test was used in 23 patients with hepatocellular carcinoma (HCC), 20 patients with breast cancer, 10 patients with prostate cancer, 20 patients with lung cancer, 20 patients with endometrial cancer tumor cells and normal tissue LHRH-R De Biaoda levels; ii) pre-tin method use direct labeling of LHRH, marking completion of saline or human serum were added at room temperature, the chromatography was measured at different times, to calculate the rate of labeled product and the radiochemical purity of the label, *in vivo* observation of its stability, and comparative analysis of selected optimal condition; iii) rat pituitary cell membrane protein, the product of *in vitro* radio-receptor marker analysis, through the saturation and inhibition experiments, was used to test its receptor binding activity; iv) Ch-T method labeled ^{125}I-LHRH, tail vein injection of normal mice at different times were sacrificed, blood and major organs were determined and calculated per gram organization percentage injected dose rate (%, ID/g). Detected by immunohistochemistry in 23 cases of HCC in the LHRH-positive rate was 82.61%, in the corresponding normal tissues, the positive rate was 15%; 20 cases of breast cancer positive rate of 95%, the corresponding normal tissues, the positive rate was 20%; 10 cases of prostate cancer positive rate of 70%, the corresponding normal tissues, the positive rate of 40%; 20 cases of lung cancer positive rate of 85%, the corresponding normal tissues, the positive rate of 15.79%; 20 cases of endometrial cancer positive rate of 80% in the corresponding normal tissues was 16.67% positive. ^{99m}Tc-LHRH mark was 97.9-100.0%, the radiochemical purity of 93.9-96.4%, marking the reaction gel content of <5%. Great product receptor marker analysis showed ^{99m}Tc-LHRH with saturable receptor binding characteristics and inhibition, and high affinity, RT = 23.2174 pmol, KD = 0.4348 nmol; intravenous injection of ^{131}I-LHRH within 72 h after the mice rapidly cleared the blood radioactivity, the major radioactive accumulation in the liver and kidneys and by the liver, renal clearance, and other tissues and organs of the radioactivity gradually decreased with time. In conclusion, i) the liver, lung, breast, prostate, endometrial cancer exist in both LHRHR; ii) ^{99m}Tc-LHRH preparation is simple, rapid, radiochemical purity product obtained higher marks, better stability, no further purification; and iii) LHRH ^{99m}Tc labeled, still has a high receptor binding ability, biological activity; and has an ideal and realistic dynamics in animals, there is hope, as with the clinical value of imaging agent of GnRH receptors.

Correspondence to: Dr Dawei Hao, Department of Radiotherapy, Xuzhou Central Hospital, 199 Jiefang Road, Xuzhou, Jiangsu 221009, P.R. China
E-mail: njp593511@163.com

Key words: target, tumor, luteinizing hormone-releasing hormone

Introduction

Worldwide, the incidence and mortality rate of cancer are on the increase, with an increasing number of young cancer patients. Early detection, early diagnosis and early treatment is the key to reducing the mortality rate. Application of many new technologies significantly increases the accuracy of early detection and diagnosis of lesions (1). Currently, exploration of the cause, development mechanisms and laws of the tumor has been elevated to the molecular and genetic level. Oncology imaging study has developed from simple anatomic description to functional imaging, molecular biology and pathophysiological development, and combined with biological markers or gene technology, can detect and determine the characteristics of the disease at the cell and molecular level (2).

Luteinizing hormone-releasing hormone (LHRH) is a decapeptide hormone, which is secreted by the hypothalamus arcuate nucleus neurons and transported by axoplasm flow of nodule-pituitary axis to nerve endings at the uplift, and then by hypophysical portal veins, it flows into the anterior pituitary gland with blood to stimulate the pituitary cells to secrete luteinizing hormone and follicle-stimulating hormone for regulating anterior pituitary gonadotropin secretion, which in turn stimulates the secretion of luteinizing hormone and follicle-stimulating hormone to regulate the level of gender hormones, in order to act on the reproductive axis and regulate the formation of gametes and gonadal endocrine (3,4). It must

be combined with high affinity transmembrane receptors to play its role, and these receptors belong to seven transmembrane receptor families (5-8). LHRH and its receptor are also found in the central nervous system (CNS) and peripheral tissues, indicating that in addition to the release of gonadotropin, this kind of decapeptide hormone also has other functions. It has been previously reported that LHRH is generated outside the hypothalamic-pituitary axis and plays specific biological effects outside the hypothalamic-pituitary axis (9). Previous findings have shown LNRH binding sites on tumor cells of ovary, breast, and endometrium, prostate and pituitary, and a high expression of LHRH-R on the tumor cells of the pancreas, lung and liver (10-17). Expression of LHRH-R in the corresponding normal tissue is relatively low. Emons *et al* first proved that approximately 80% of ovarian cancer tissues possess binding sites of specificity LHRH, LHRH agonist or antagonist analogues, which indicated the existence of the high affinity LHRH receptor in human ovarian cancer (7). Some LHRH agonists have been used in the treatment of ovarian cancer. Eidne *et al* first proved the existence of LHRH binding sites on human breast cancer cells (18). Subsequent literature reported the MTX mouse breast cancer cell nuclei has LHRH-R distribution (19). Human breast cancer cell lines MDA2MB2231 and ZR27521 cell extracts cultured *in vitro* showed LHRH immunoreactive (20). Rusiecki *et al* observed LHRH receptor expression in breast cancer and tissues adjacent to cancer and the relationship between LHRH receptors, estrogen (ER), and progesterone receptor (PgR). The study selected pathological tissue of 90 cases of breast cancer patients, and randomly selected 40 cases of normal tissue adjacent to normal tissue (45 vs. 39%), the results showed that LHRH-R expression is related to tumor tissue with positive PgR (21). In addition, LHRH-R expression of premenopausal breast cancer patients without menstruation is higher (56 vs. 32%, the latter is the value of normal humans) (22). Although LHRH analogues for the treatment of endometrial cancer has a long history, the study on LHRH and its receptor expression in endometrial cancer tissue has just started in recent years, and study of its therapeutic mechanism has been a hotspot over the past 2-3 years. Imai *et al* found that LHRH stimulation can induce apoptosis in some human reproductive tract tumor cells mediated by Fas ligand. The incidence of primary liver cancer has a significant gender difference (male:female = 9:1 to 7:1), and experimental study and clinical observations have suggested that liver cancer may be a hormone-dependent tumor (23). Recently, LHRH-R gene in human hepatocellular carcinoma (HCC) has been successfully cloned, with investigators confirming that the complementary DNA libraries of LHRH and its receptor produced by PCR reaction and human placenta and pituitary gland LHRH receptor are identical through DNA blot analysis with endogenous oligonucleotide primers as a probe (24). This shows that, LHRH and LHRH-R non-germline mRNAs are widely distributed in normal or malignant tissues that do not belong to reproductive system (25,26). The adjacent piece immunohistochemical double labeling method also shows LHRH in HCC may regulate the growth and differentiation of liver cancer cells in autocrine manner (OS). Katsuno *et al* found the expression of LHRH on hypophysis growth hormone cell tumors by means of immunohistochemistry and *in situ* hybridization (27). Some researchers have applied LHRH to the clinical treatment of pituitary adenomas, and found that after a long-term treatment (6 months), pituitary tumor was significantly reduced. This suggests that LHRH can inhibit the growth of pituitary tumor cells (28). The above facts show that normal human pituitary and pituitary tumor cells can express LHRH and its receptor, and that LHRH in pituitary tumor cells may act as an autocrine or paracrine regulator to fulfill its function (28,29). Among tumors derived from non-gonadal axis, pancreatic cancer is a malignant tumor relatively closely connected to LHRH. It has been demonstrated that there are LHRH-R distribution on hamster pancreatic cancer tissue induced by N-dinitroso dioxopropyl two amines (BOP) and human pancreatic tissue through autopsy; and no LHRH binding sites was detected on normal hamster and human pancreatic cancer tissue (30). Szepeshazi *et al* (31) applied bombesin gastrin-releasing peptide (GRP) agonist RC23095, growth hormone releasing somatostatin analogues RC2160 or LHRH agonists cetrorelix to hamsters induced by nitrite, 8 weeks later, they discovered that epidermal growth factor (EGF) expression in carcinoma tissue decreased by 71 and 69%, respectively. This indicates that EGF may be involved in the adjustment of inhibitory effect LHRH exerts on pancreatic tumor cell growth (32,33).

The identification of LHRH analogs (LHRH-a), activator (LHRHag), and antagonist (LHRHanta) has promoted the study on physiological function of LHRH and its receptor. LHRH is a neurotransmitter in the CNS and the sympathetic nervous system; a paracrine regulator in the gonads and placenta; an autocrine regulator in some tumor cells (19,34,35). Human LHRH-R is composed of 328 amino acids and 7 transmembrane domains, which belongs to G protein-coupled receptors. Junction station of LHRH-R and LHRH in mammalian pituitary gonadal cells has high specificity (36). Photoaffinity labeling, and chromatographical electrophoresis have proved that LHRH-R is a glycoprotein of M-6000, and has 3 N-glycosylation sites, the possible interaction between acidic amino acids at 90, 98 and 29 and arginine in LHRH enables LHRH to play its physiologic adjustment function (37). LHRH-R can also be generated and expressed in hypothalamic-pituitary axis, for example, LHRH-R mRNA expression can be found on human ovarian granulosa, luteal cells, testicular interstitial cells, breast tissue, prostate and rat gastrointestinal epithelium and glandular epithelial cells, suggesting that these LHRH target organs can synthesize LHRH-R by themselves. The presence of LHRH or analogue activates LHRH-R to perform different functions by G protein-coupled phosphoinositide pathway and mediated calcium mobilization, for instance, LHRH in the digestive tract and circular blood may be a sort of gastrointestinal hormone, which can not only play an indirect regulation through the vagus nerve on functions of gastrointestinal system, but also plays a direct role in the regulation of the digestive system through the binding with LHRH-R on mucosal epithelium and epithelial cells (38-40).

Studies over the past decade also found that, LHRH and its receptors are involved in the occurrence and development of some tumors, especially certain tumors with the non-gonadal axis organ origin. For example, LHRH-R also exist in lung cancer, kidney cancer and liver cancer cells. Previous findings showed that LHRH-R expression in gland cancer cells may

be a common phenomenon (41). Additionally, it was identified that, LHRH and its receptor inhibits proliferation of cancer cells, whose expression is closely related to differentiation degree of cancer tissue, i.e., the higher the differentiation degree, the higher the expression of LHRH and its receptors, whereas, the poorer the differentiation degree, the lower the LHRH and its receptor expression (42).

There is evidence showing that LHRH can directly inhibit the proliferation of certain hormone-sensitive tumors, and although it is known that such physiological stimuli leading to cell death is firstly achieved by apoptosis, its antitumor molecular mechanism remains unclear. Some scholars believe, LHRH inhibitory effect on tumor is realized by a mechanism independent of the release of pituitary gonadotropin. Nevertheless, antitumor effect and its targeted therapeutic value of LHRH and its analogues have been widely demonstrated in clinical applications. Studies have reported that the treatment of malignant tumors with high expression of corresponding receptors by combining LHRH targeting with biological toxins or nanoparticle technology has been used in clinical application (32,33).

High expression of a variety of aforementioned pathological conditions provides a basis for using LHRH receptor for imaging. However, studies on LHRH receptor imaging applied to cancer diagnosis are scarce. There is some literature on the characteristics of labeling method and labeled product of radionuclide-labeled LHRH of ^{68}Ga, ^{123}I, ^{18}F, ^{99m}Tc, some labeled products have entered the pharmacological evaluation stage; there is other literature examining the possibility of the corresponding labeled product serving as developing agent in SPECT, PET imaging, some findings suggested that LHRH would have a broad prospecting receptor imaging of malignant tumors with high corresponding receptor expression (34). However, most such studies still remain at the stage of labeling conditions and involve no further study of malignant tumor cells with high corresponding receptor expression.

Application basis of LHRH receptor imaging in cancer diagnosis lies in the number of expression of tumor cell LHRH-R, as well as specificity level of its combination with LHRH. This study employs immunohistochemical method to detect LHRH-R expression level in tumor cells and normal tissues; pre-tinning to directly label LHRH, measuring and calculating labeling rate and radiochemical purity of labeled product, observing its stability *in vivo* and *in vitro*, and selecting labeling method and its optimal condition with higher radiochemical purity and sound stability through comparative analysis. Normal mice were used for live animal experiment to detect the expression levels in tissues and organs of normal live animals as well as metabolism of radio-labeled LHRH *in vivo* of live animals. The value of LHRH-R expression in tumor cells and LHRH receptor imaging in targeting diagnosis of tumors provided theoretical and experimental basis for further study.

Materials and methods

LHRH-R expression in tumor and normal tissue

Specimen collection. Paraffin specimen of related tumors were collected. Criteria of inclusion were as follows: i) Tissue blocks were fixed in 10% formalin and embedded in paraffin in a routine manner, and were sliced into several sections at the thickness of 4 μm; ii) none of the patients had received preoperative radiotherapy and chemotherapy; iii) surgical treatment were radical resection and tumor-free margins exist; and iv) the pathological diagnosis complied with classification criteria of WHO lung cancer histology in 1998, which did not include small cell lung cancer, carcinoid tumors and metastatic cancer. Qualified cancer tissue samples in the group were 93 cases, including 10 cases of prostate cancer, 20 cases of breast cancer, 20 cases of endometrial cancer, 23 cases of liver cancer and 20 cases of lung cancer.

Treatment of specimens

Treatment of slides. Fresh slides were immersed in cleaning solution for 24 h, rinsed with clean water for 2 h, washed 3 times with distilled water, and place in oven at 37˚C after clean rinsing, soaked in 1:10 poly-L-lysine for approximately 10 sec, drained and placed in oven at 37˚C. All the specimens were confirmed by pathology.

Treatment of specimen slices. The specimens were fixed in 10% formalin and embedded in paraffin, and were sliced into several pieces at 4 μm, and placed at 37˚C incubator for 2 h for standby application.

Control setting. With phosphate-buffered saline (PBS) substituting primary antibody as negative control, the remaining steps were unchanged.

Immunohistochemical staining procedure. Paraffin sections were dewaxed in xylene and hydrated with graded alcohol, and then were washed with PBS (pH 7.4) 3 times, each time for 3 min. The sections were placed in freshly-prepared boiled (pH 6.0) citrate buffer for antigen retrieval. To each slice was added a drop of 3% hydrogen peroxide solution, and incubated at room temperature for 15 min, so as to block endogenous peroxidase and was washed with PBS 3 times, each time for 3 min.

After tossing PBS solution, to each slice was added with a drop of primary antibody (1:200 dilution), overnight at 4˚C. Blank control used primary antibody in place of PBS. The slice was washed with PBS 3 times, each time for 5 min. After removing PBS solution, to each slice was added a drop of polymer enhancer (reagent A), and incubated at room temperature for 20 min. PBS rinsing followed 3 times, each time for 3 min.

After removing PBS solution, each slice was added a drop of anti-rabbit HRP polymer (reagent B), and incubated at room temperature for 30 min. PBS rinsing was 3 times, each time for 3 min.

After removing PBS solution, each slice was added with a drop of freshly-prepared DAB coloration liquid, and observed under the microscope for 3 to 5 min, positive coloration is brown, using tap water for rinsing to terminate the coloration.

The slices were rinsed with distilled water and redyed with hematoxylin using 0.1% hydrochloric acid to differentiate and tap water to rinse the slices, and then stained blue. Employing graded alcohol to dehydrate, xylene for transparency, and mounting with neutral gum. Elivision reagent kit contained the reagents A and B.

Immunohistochemical results. LHRH-R positive coloration occurred mainly on cancer cell cytoplasm taking on

brown particles. Immunohistochemistry using semi-quantitative scoring method for determination, i.e., the overall score was calculated according to staining intensity and the percentage of number of positive cells in total number of tumor cells.

Rating according to the degree of positive staining: 0, no coloring, consistent with the background color; 1, pale yellow, slightly higher than the background color; 2, claybank, significantly higher than the background color; and 3, brown.

Rating according to the percentage of positive cells: 0, negative; 1, <10%; 2, 11-50%; 3, 51-75%; and 4, >75%.

The product of the two was calculated to determine the positive result: 0-2 indicated negative (-); 3-4 indicated weak positive (+); 5-8 indicated moderately positive (++); and 9-12 indicated strong positive (+++).

Using pre-tinning ^{99m}Tc to directly label LHRH

Labeling method. After adding 0.1 ml of sodium gluconate (0.3 mol/l, dissolved by PBS buffer), 0.05 ml of stannous chloride that was dissolved by concentrated hydrochloric acid (40 mg/ml), 0.1 ml of $^{99m}TcO_4^-$ physiological saline eluent, and 0.1 ml of PBS buffer into the reaction tube, it was placed at room temperature for 10 min after being mixed in vortex mixer. Na_2OH was used to set pH at 3.0, and 10 μg LHRH was added. Placing it in a constant temperature water bath at 40˚C for 1 h. The labeling was completed.

Changing labeling conditions. i) Labeling under the circumstances of using sodium gluconate as the complexing agent and without the complexing agent, respectively; ii) dosage of stannous chloride and the pH of the reaction system were changed, respectively, changing, dosage of $SnCl_2$ increased from 20 to 60 mg/ml, pH of the reaction increased from 2.0 to 4.0; and iii) the reaction temperature increased from 25 to 50˚C.

Stability in vitro. ^{99m}Tc-LHRH was added to fresh saline and normal human plasma (37˚C), respectively, and mixed, and then radiochemical purity was measured at 30 min, 1 h; 90 min, 2, 3 and 4 h.

Determination of radiochemical purity. No. 1 Xinhua chromatography paper was used as stationary phase, and saline as mobile phase to measure radiochemical purity (development system I); no. 1 Xinhua chromatography paper soaked in 2.5% bovine serum albumin (BSA) was adopted as stationary phase, and ethanol developing solvent:ammonia:water = 2:1:5 to measure colloid (development system II), and GC-300γ counter was employed to measure radioactivity.

Result criteria. In development system I, the free ^{99m}Tc went to the leading edge with the expansion of solvent (Rf = 1.0), while the colloid and marker remained at the original point (Rf = 0); in eluent II, the colloid was maintained at the origin (Rf = 0), while the free ^{99m}Tc and markers migrated to the forefront along with the solvent (Rf = 1.0); eluent I and II system could completely distinguish ^{99m}Tc-LHRH, colloids and free ^{99m}Tc in this study. The finally obtained radiochemical purity of ^{99m}Tc-LHRH exceeded 90%, and colloid content was <10% indicating successful labeling.

^{99m}Tc-LHRH receptor binding in vitro

Preparation of rat pituitary cell membrane protein. The whole experiment process was set in an ice bath. Pituitary was quickly removed after the sacrifice of Sprague-Dawley (SD) rats, and rinsed in an ice bath of pH 7.4 10 mmol/l Tris-HCl (containing 0.5 mmol/l PMSF, adding PMSF, 1.2 mmol/l $MgCl_2$, 0.01 mmol/l EDTA-Na_2 before using) twice to remove blood.

The pituitary was set inside the electric glass homogenizer for homogenizing after the rinsing (2,000 rpm, 10 sec x 3 times), and centrifuged at 4˚C (2,000 x g, 5 min). After discarding the sediment, the supernatant was centrifuged again at 4˚C (20,000 x g, 20 min), then supernatant was discarded and the sediment was rinsed 10 times the volume of Tris-HCl twice (20,000 x g, 20 min), thus, the rat pituitary cell membrane protein was attained. A small amount of Tris-HCl suspension was added. BCA protein assay kit was employed to measure absorbance values at 562 nm on a microplate reader. According to the standard curve scheme membrane protein concentration, protein concentration was adjusted to 2 mg/ml, and placed at -70˚C for cryopreservation separately.

Receptor assay. The 12x75 mm test tube was taken and prepared with 1% BSA (Tris-HCl, pH 7.4 preparation) before using (BSA was added to the tube, and kept overnight at 4˚C, and then BSA was emptied, and the tube was inverted for standby application).

All the tubes were added with 50 μl of rat pituitary membrane proteins (100 μg), including sub-unit binding tube (TB) and nonspecific binding (NSB) tubes, then followed by 2, 5, 10, 20, 30, 40 and 50 μl of ^{99m}Tc-LHRH. NSB tubes were added with 2 μg gonadorelin (prepared with Tris-HCl to ensure there were much more gonadorelin than ^{99m}Tc-LHRH in NSB tube), and finally the reaction volume was complemented to 150 μl with Tris-HCl (this buffer was made by adding 0.2% BSA to protein-extraction buffer, pH 7.4).

The tubes were incubated at 37˚C set oscillator for 1 h and were added 1 ml precooled Tris-HCl at 4˚C after the removal. The reaction was quenched by mixing. The left reactant was collected on glass fiber filter paper 49 with multi-point cell harvester (ZT-II type), and the reaction tube was added Tris-HCl and washed 3 times (1 ml/time), and finally 1 ml 5% TCA filter paper was placed in the test tubes. Measurement of radioactivity of each tube was counted with γ tube immune counter, as well as TB and NSB.

Measured results employed SB/FREE as the vertical axis, the amount of specific binding SB as the abscissa, and Scatchard plot, equilibrium dissociation constant KD was attained, SB (dpm) = TB (dpm) - NSB (dpm), unbound ^{99m}Tc-LHRH F (dpm) = added ^{99m}Tc-LHRH T (dpm) - total binding TB (dpm).

LHRH metabolisms in vivo

Preparation of ^{125}I-LHRH.

Chloramine-T method to label LHRH. 4 mCi ^{125}I/0.4 μl, LHRH 10 μg/10 μl, and 50 μg chloramine-T were added into Eppendorf (EP) tube successively. The mixed solution was left to react for 90 sec (during the reaction, the solution was shaken on the vortex mixer), then 100 μg $Na_2S_2O_5$ was added and the solution was mixed on the vortex mixer, finally the reaction was terminated. The labeling was completed.

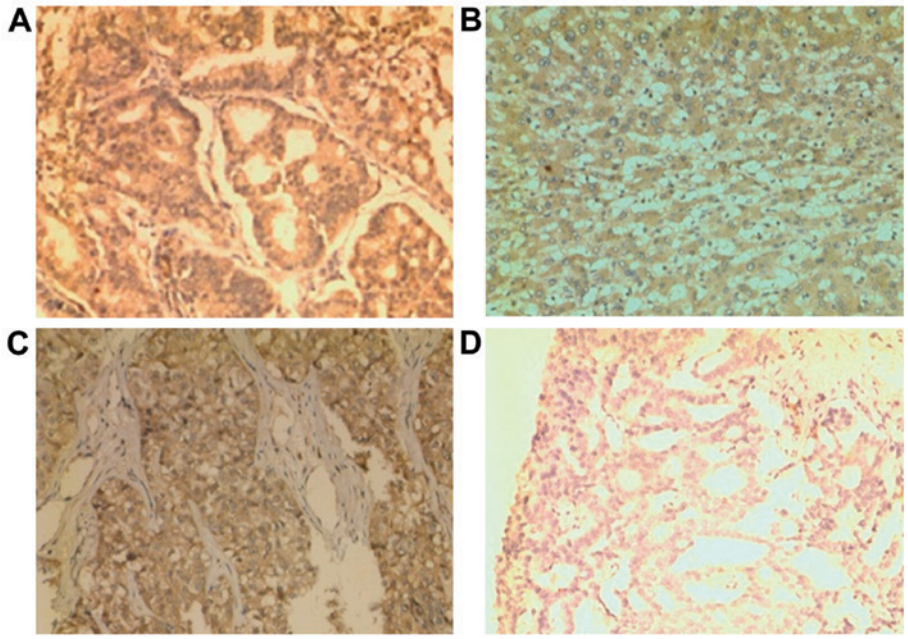

Figure 1. Immunohistochemical staining of LHRH in different tissues (10x10). (A) Lung adenocarcinoma; (B) hepatic ocarcinoma; (C) breast cancer; and (D) endometrial cancer. LHRH, luteinizing hormone-releasing hormone.

Production of Sepahdex G-25 gel column. After the G-25 gel particles were immersed into pure water for 24 h, they were added into glass acid buret containing glass fiber at the bottom. After the air was exhausted, using 10 column volumes of PBS buffer to rinse slowly, then 10 ml 1%. The BSA saturated gel column was added.

Separation and purification of ^{125}I-LHRH. ^{125}I-LHRH was added into Sepahdex G-25 gel column, and the reaction tube was washed with PBS 2 times, each time 100 μl, gel column was also added, and was rinsed slowly with PBS. Dripping speed was adjusted to 6 drops/min, and leaching liquid solution was collected (1 ml/tube). Employing paper chromatography to measure its radiochemical purity, respectively (no. 1 Xinhua paper chromatography paper was used as stationary phase and the normal saline as the mobile phase, γ counter was used to measure radioactivity count). The highest radiochemical purity was taken for further experiments.

Animal experiments. Forty-five healthy male mice aged ~23 weeks and weighing 20±2 g were divided into 9 groups according to random number table, with each group including 5. The 54.1 mCi/100 μl ^{125}I-LHRH was injected into tail vein. A group of mice was taken, respectively, 15 and 30 min, 1, 2, 4, 6, 24, 48 and 72 h after the injection. Blood was collected from picked eyeballs. Using stem dislocation to sacrifice the mice and then they were dissected, major organs (heart, lungs, liver, spleen, kidney, muscle, bone, brain, small intestine and stomach) were taken and weighed. γ counter was used to measure radioactivity count of blood and organs, and unit mass of tissue percentage radioactivity uptake dose rate (%, ID/g) was calculated (per gram of tissue radioactivity count/total radioactivity injected into mice count x 100%).

Statistical analysis. Data are presented as mean ± standard deviation (mean ± SD). SPSS 16.0 statistical software (SPSS, Inc., Chicago, IL, USA) was used for Fisher's exact test. P<0.05 was considered to indicate a statistically significant difference.

Table I. The expression of LHRH in tissues.

Pattern of tissues	n	No. of positive cases	Positive rate (%)	P-value
Lung cancer	20	17	85	P<0.05
Peritumoral lung tissue	19	3	15.79	
HCC	23	19	82.61	P<0.05
Adjacent liver tissue	20	3	15	
Breast cancer	20	19	95	P<0.05
Peritumoral breast tissue	20	4	20	
Endometrial cancer	20	16	80	P<0.05
Peritumoral endometrial tissue	18	3	16.7	

The Fisher's exact test was conducted, and tumor group and control group (peritumoral tissue) were compared, P<0.05. LHRH, luteinizing hormone-releasing hormone.

Results

Immunohistochemical staining. Immunohistochemistry of specimens had good stain specificity. Pale background or blank background. Positive product of immunoreaction was brown. As contrast was obvious, it was easy to confirm. Immunohistochemical staining results of LHRH in different tissues are shown in Table I and Fig. 1A-H.

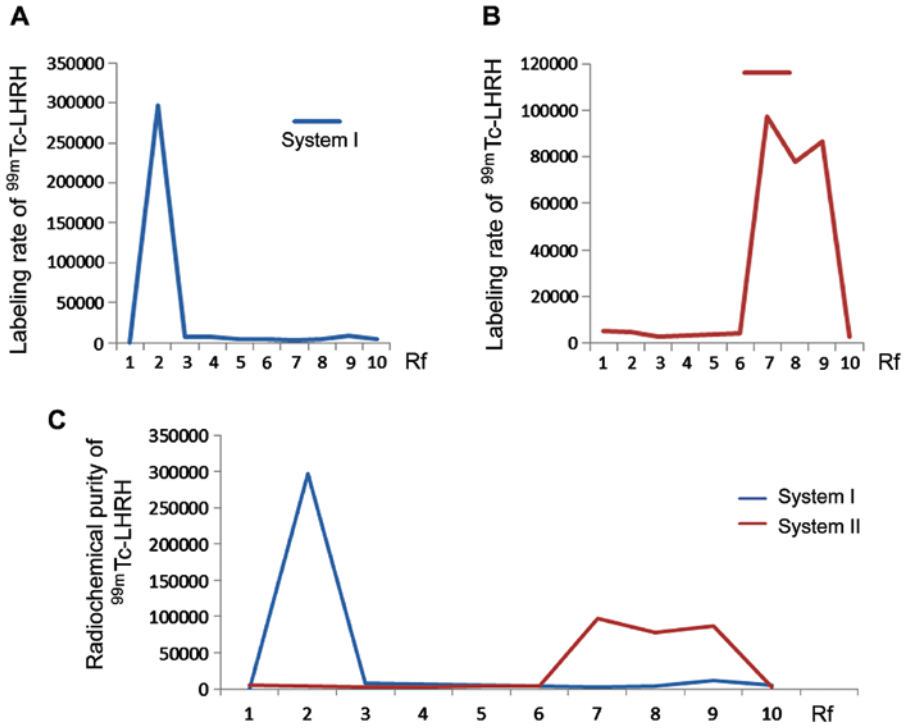

Figure 2. Labeling rate and radiochemical purity of ^{99m}Tc-LHRH. (A) Development system I; (B) development system II; and (C) the labeling rate of paper chromatography and the content of colloid. LHRH, luteinizing hormone-releasing hormone.

Labeling rate and radiochemical purity of ^{99m}Tc-LHRH. In development system I, the free ^{99m}Tc went to the leading edge with the expansion of solvent (Rf = 1.0), while the colloid and marker remained at the original point (Rf = 0); in eluent II, the colloid was maintained at the origin (Rf = 0), while the free ^{99m}Tc and markers migrated to the forefront along with the solvent (Rf = 1.0); eluent I and II system could completely distinguish ^{99m}Tc-LHRH, colloids and free ^{99m}Tc in this study. The highest LHRH labeling rate by employing direct method of no. 1 Xinhua paper chromatographic hit (98.7±0.93%); the highest radiochemical purity reached 95.2±1.02% (Fig. 2A-C).

Impact of complexing agent. In the case of no complexing agent was used, the presence of white sediment in the reaction system signified unsuccessful labeling. With 0.1 ml of sodium gluconate (0.3 mol/l) as complexing agent, when pH value stood at 3.0, the radiochemical purity was up to 95.2±1.02%, colloid content in the labeling reaction was <5%.

Impact of $SnCl_2 \cdot 2H_2O$ dosage and pH value on radiochemical purity. In case that other labeling conditions (volume of ^{99m}Tc eluent, reaction temperature, peptide dosage) remained the same, $SnCl_2 \cdot 2H_2O$ and pH value were changed, resulting radiochemical purity is shown in Table II.

Effect of reaction temperature. In case that other labeling conditions (volume of ^{99m}Tc eluent, $SnCl_2 \cdot 2H_2O$ dosage, pH value and peptide dosage) remained the same, the reaction temperature was changed. At 25˚C, the radiochemical purity was 32.6±1.9%, at 40˚C, it was 91.6±3.5%, at 50˚C, it was 57.8±1.9%.

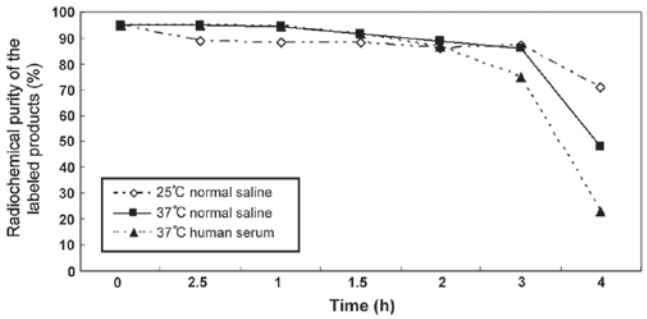

Figure 3. Stability of the labeled products *in vitro*.

Stability in vitro of labeled product. Within 3 h, reactants maintained a high radiochemical purity and declined sharply after 3 h (Table III and Fig. 3).

In vitro binding of ^{99m}Tc-LHRH receptor. Receptor saturation analysis showed that total combination increased with ^{99m}Tc-LHRH and specific binding rose quickly at the outset. When ^{99m}Tc-LHRH was increased to a certain amount, the curve flattened and stopped increasing, and showed saturation trend, indicating that the receptor has been absorbed by ^{99m}Tc-LHRH. NSB increased linearly with ^{99m}Tc-LHRH, showing no saturation trend (Table IV and Fig. 4A). With B/F as the vertical axis, the binding capacity as the abscissa, and figure was drawn by Scatchard plot, RT = 23.2174 pmol, KD = 0.4348 nmol (Fig. 4B).

Distribution of ^{125}I-LHRH in normal mice. Distribution result in normal mice can be seen in Fig. 5. ^{125}I-LHRH was injected into the mouse tail vein, 15 min later, blood radioactivity was

Table II. Impact of $SnCl_2 \cdot 2H_2O$ dosage and pH value on radiochemical purity (%).

	pH value				
$SnCl_2 \cdot 2H_2O$ (μg)	2	2.5	3	3.5	4
1,500	65.1±3.2	57.6±1.6	58.1±1.3	60.4±2.1	49.3±1.3
2,000	83.8±0.9	83.5±2.7	93.9±1.0	88.4±0.8	72.4±3.7
2,500	75.1±2.4	82.8±2.0	64.9±4.0	60.7±1.1	[#]

[#]White sediment appeared.

Table III. Stability *in vitro* of labeled product.

Degrees	0 h	0.5 h	1 h	1.5 h	2 h	3 h	4 h
25˚C saline	95.2±1.023	88.7±2.472	88.1±3.556	88.1±3.044	86.2±2.434	87.3±2.055	71.2±2.575
37˚C saline	95.2±1.023	95.0±1.466	94.2±1.563	91.7±0.634	89.0±2.677	85.8±10.537	48.2±2.423
37˚C human serum	95.2±1.023	95.1±1.359	94.4±0.249	91.4±1.178	86.4±1.744	74.6±2.439	23.0±3.146

Table IV. Experiment data of *in vitro* binding of ^{99m}Tc-LHRH receptor.

Protein nos. (μl)	Total count (T)	Total binding count (TB)	Count of non-specific (NSB)	Count of specific binding (SB)	Corresponding LHRH amount of binding (pmol)	B/F
2	12,742	1,088	587	501	3.9318	0.04299
5	31,855	1,795	714	1,081	8.484	0.03596
10	63,710	2,465	923	1,542	12.1016	0.02518
20	127,420	3,462	1,367	2,095	16.4416	0.0169
30	191,130	4,056	1,678	2,378	18.6625	0.01271
40	244,840	4,575	2,176	2,399	18.8274	0.009985
50	318,550	4,835	2,486	2,349	18.435	0.007488

LHRH, luteinizing hormone-releasing hormone.

up to 3.09% ID/g, which was then quickly cleared, and 4 h later, it reduced to <1% ID/g; radioactivity distribution in kidneys was high, and peaked at 9.24% ID/g after 15 min, then decreased rapidly, and 1 h later, it decreased to 1.35% ID/g, followed by a rapid rise to 5.85% ID/g again, and then gradually cleared away; liver also had a high radioactivity uptake, and 15 min later, it reached 5.79% ID/g, which may be associated with blood perfusion and nonspecific uptake, and then was removed quickly; gastrointestinal uptake was relatively high at the outset, and peaked 2 h later at 6.69% ID/g and 4.50% ID/g, respectively. Radioactivity in heart, lung, spleen, brain, bones and muscles decreased over time.

Discussion

In this study, by using immunohistochemistry assay, LHRH positive rate in 23 cases of HCC was 82.61%, and positive rate of corresponding normal tissues was 15%; positive rate of 20 cases of breast cancer reached 95%, and positive rate of the corresponding normal tissues was 20%; positive rate of 10 cases of prostate cancer, was 70%, while positive rate of corresponding normal tissues was 40%; positive rate of 20 cases of lung cancer was 85%, and positive rate of corresponding normal tissues reached 15.79%; positive rate of 20 cases of endometrial cancer was up to 80%, and positive rate of corresponding normal tissues was 16.67%. Expression amount of LHRH-R in tumor cells constituted the application basis of LHRH receptor imaging in cancer diagnosis, while high expression of LHRH-R in these tumor tissues and significant expression differences compared with their corresponding normal tissues provided the foundation for using LHRH body imaging.

Peptide radioactive agent has many advantages: Ligand peptide is chemically synthesized, which overcome the heterogeneity problem, and almost does not incur human immunogenicity response; its low molecular weight makes

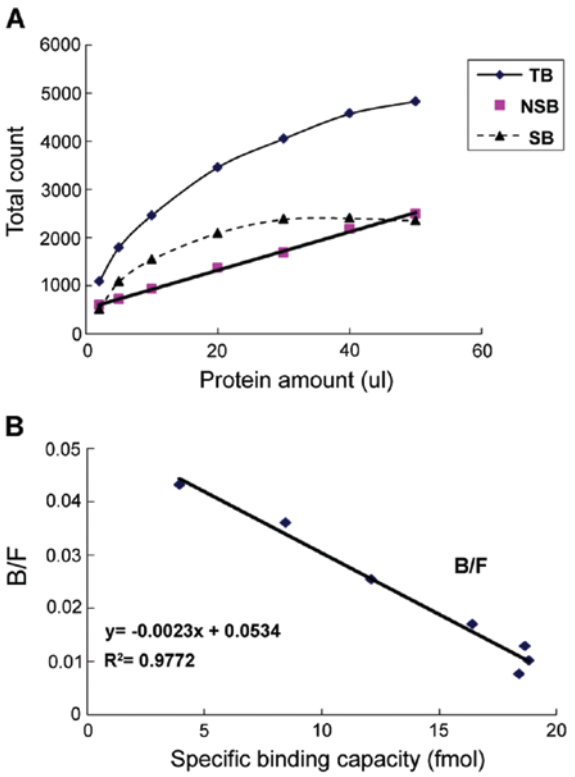

Figure 4. *In vitro* binding of ^{99m}Tc-LHRH receptor. (A) ^{99m}Tc-LHRH saturation binding experiment; and (B) ^{99m}Tc-LHRH Scatchard plot saturation binding experiment. LHRH, luteinizing hormone-releasing hormone.

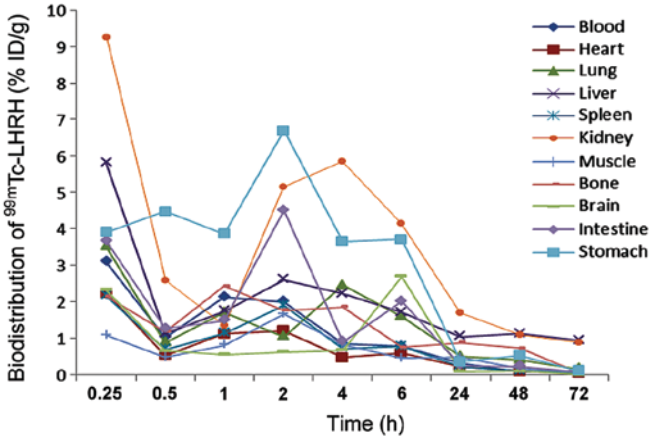

Figure 5. Distribution of ^{99m}Tc-LHRH in the body of normal rats (mean ± SD, n=5). LHRH, luteinizing hormone-releasing hormone.

it easy for peptides to get through physiological barrier and penetrate tissues, and it can reach target and clear away blood quickly, which helps to reduce radioactive background and improve tumor/non-tumor (T/NT) ratio (43), therefore high-contrast tumor imaging can be obtained in a relatively short time.

LHRH-R shows high expression in a variety of tumor cells. Using appropriate radionuclide to label LHRH analogues is conducive to early diagnosis and treatment of related cancer. There are now a number of radionuclides for marking LHRH analogues (44).

Chloramine-T methods most commonly used to label LHRH with iodine. Radioactive iodine (such as ^{123}I/^{125}I/^{131}I) is labeled on the 5th tyrosine of LHRH. The labeling process is simple with mild reaction conditions (45). After the labeling, separation and purification of free iodine and iodine binding peptides must be conducted, which takes a long time, and because the iodine connected to tyrosine is easy to fall off in the body and ^{123}I is expensive, the application of iodine-labeled LHRH is rare (46,47).

^{18}F labeled-LHRH mostly uses indirect labeling method. ^{18}F often causes deformation to LHRH molecular structure, thereby affecting its biological activity, so labeled prosthetic groups or the so-called bi-functional ligands are widely used to connect radionuclides and biologically active molecules (31). However, such labeling methods often have various radioactive steps and long duration (36).

Relative to other radionuclides, ^{99m}Tc possesses moderate energy, and its gamma-ray energy is 140 keV, which is readily available and of low cost. It can be easily obtained through ^{99}Mo-^{99m}Tc generator, which is currently the most commonly used clinical radionuclide. Main methods of using ^{99}Mo-^{99m}Tc to label polypeptides are as follows: i) Indirect labeling method carried out by chelating agent; ii) direct reduction method; and iii) using biotin and avidin system to label (48). Currently, modified Schwartz method and pre-tinning method are frequently used (31). In this study, pre-tinning was adopted to directly label LHRH, and adding sodium gluconate in the reaction system as a complexing agent, in order to prevent the formation of Sn-colloid, Tc-colloid and Sn-Tc colloid. By altering pH value of reaction system, reaction temperature and the amount of reducing agent, labeling rate and radiochemical purity of ^{99m}Tc-LHRH under different conditions were compared, the resulting labeling rate of optimal labeling method was 97.9-100.0%, radiochemical purity was up to 93.9-96.4%, and colloid content in the labeling reaction was <5%. The method is simple with the high radiochemical purity of the resulting product. Although 3 h after being placed in 37˚C human serum, the radiochemical purity dropped to ~75%, but 2 h later, it was still nearly 90%. Given that in the present clinical study, imaging often occurs 2 h after the introducing imaging agent, ^{99m}Tc-LHRH obtained by this method may become imaging agent for LHRH-R positive tumor receptors.

Moreover, ^{99m}Tc-LHRH has receptor binding characteristics, which is a basic condition for receptor imaging agent. In receptor analysis, plenty of gonadorelin was added into NSB, this peptide served as LHRH antagonist, three receptor analysis revealed radioactivity counting measurement of each NSB tube took on linear relationship with corresponding ^{99m}Tc-LHRH, and all exceeded 0.90, suggesting that because at this time substantial amount of gonadorelin membrane proteins occupied LHRH-R sites in pituitary, measurement of each tube took on linear relation, which indicated that these counts were combination of ^{99m}Tc-LHRH, miscellaneous proteins in the cell membrane, and test wall rather than count formed by its binding to the receptor, i.e., NSB. In TB tube, because there was no LHRH, radioactive counts of each tube consisted of two parts, one part of count was formed by ^{99m}Tc-LHRH binding to its receptor (i.e., SB), and one part was the NSB count of ^{99m}Tc-LHRH, therefore SB

was obtained through TB-NSB. The count of each TB tube increased rapidly as the amount of ^{99m}Tc-LHRH increased, indicating that the receptor had a surplus, then the count gradually increased, indicating that the receptor binding was basically complete, and the count increased simply because of the NSB.

The SB obtained showed similar curves with TB, and although TB curve later rose slowly, it still increased as ^{99m}Tc-LHRH went up, but at certain time SB curve flattened, showing that receptors were saturated. Usually, affinity between receptor and ligand is bound by 10^{-9}, KD $\geq 10^{-8}$ indicating the low affinity between receptor and ligand, the bigger the KD, the lower the affinity, and KD $\leq 10^{-9}$ indicated high affinity between ligand and receptor, which belongs to high affinity ligand, the smaller the KD, the higher the affinity. In this study, by external cell membrane protein receptor saturation binding experiment, it was confirmed that ^{99m}Tc-LHRH could be suppressed by LHRH, RT = 23.2174 pmol, KD = 0.4348 nmol, which indicated the labeled ^{99m}Tc-LHRH was the low-capacity and high-affinity ligand of the receptor. Affinity was similar to 0.4792 nmol, KD value of carcinoembryonic cell receptor obtained by predecessor who used ^{99m}Tc-LHRH, but lower than 10 nmol, KD value obtained by Barda *et al* who analyzed the combination of external binding between ^{99m}Tc-LHRH and receptor in rat pituitary cell membrane (19). Probably differences in tissue origin of receptor specimens and preparation methods, as well as employed LHRH structure caused the figure discrepancy. Receptor analysis demonstrated that ^{99m}Tc-LHRH was the receptor's high affinity ligand, i.e., ^{99m}Tc-LHRH and unlabeled LHRH had a high affinity for its receptor, and its biological activity and receptor affinity was unaffected, which also provided an experimental basis for ^{99m}Tc-LHRH as receptor imaging agent for LHRH-R positive tumors.

In vivo metabolism experiment of ^{125}I-LHRH in a live animal showed that after intravenous injection of ^{125}I-LHRH in the tail, blood radioactivity of the mice reached a maximum of 3.09% ID/g after 15 min, then quickly faded away, and 4 h later the figure was <1% ID/g, which helped to reduce the background and increase the target/non-target tissue radioactivity ratio; distribution of radioactivity in kidneys was very high, and peaked at 9.24% ID/g after 15 min, but followed by a rapid decrease, and after 1 h, the figure was 1.35% ID/g, and then again rapidly increased to 5.85% ID/g, then gradually faded away. The first peak indicated the high perfusion of kidney tissue after the tail vein was injected with ^{125}I-LHRH, and the second peak suggested that the imaging agent was mainly excreted through the urinary system, which was conducive to the detection of chest and abdominal tumor; liver and lungs also had a higher uptake, which peaked at 15 min and may be associated with blood perfusion and non-specific uptake, followed by rapid clearance. Immunohistochemical results showed normal liver and lung tissue has a certain amount of receptor expression, but receptor expression in the tumor was much higher than that in normal tissue, which was conducive to the detection of liver and lung tumors; gastrointestinal radioactivity uptake was relatively high at the outset, peaked at 2 h, which was 6.69% ID/g and 4.50% ID/g, respectively. On one hand, it showed that there were certain amounts of LHRH-R expression in gastrointestinal tissue; on the other hand, it showed that part of marker was excreted from the digestive tract, hence it was not suitable for the detection of gastrointestinal cancer. ^{125}I-LHRH in heart and spleen mainly took on blood pool type distribution, and its concentration decreased with clearance of the blood background. Brain, bone and muscle radioactivity decreased over time.

In conclusion, positive rate of LHRH-R expression in human liver, lung, breast, prostate, endometrial tumors is significantly higher than that in adjacent normal tissue, and difference in expression intensity compared with the normal control group is statistically significant. Studies have shown that this labeling method is fast and easy, and the resulting radiochemical purity of the labeled product is relatively high, which does not call for further purification and has good stability. ^{99m}Tc-LHRH labeled by this method has high affinity in its binding with its receptor and its biological activity and receptor affinity is not significantly affected. Radionuclide labeled LHRH has an ideal kinetics performance in the body of animal, which holds promise for an imaging agent of clinically practical value of LHRH receptor.

References

1. Yuan B, Zhang J and Zhang YQ: Research progress of relation between GnRH and its receptor and tumors. Prog Anatomical Sci 8: 367-371, 2002 (In Chinese).
2. Jia PY and Wang YX: Application of gonadotropin-releasing hormone and its receptor in cancer therapy. J Int Pharm Res 36: 179-183, 2009 (In Chinese).
3. Yin H, Cheng KW, Hwa HL, Peng C, Auersperg N and Leung PC: Expression of the messenger RNA for gonadotropin-releasing hormone and its receptor in human cancer cell lines. Life Sci 62: 2015-2023, 1998.
4. Wen S, Schwarz JR, Niculescu D, Dinu C, Bauer CK, Hirdes W and Boehm U: Functional characterization of genetically labeled gonadotropes. Endocrinology 149: 2701-2711, 2008.
5. Xie J: The current development and prospect of tumor molecular nuclear medicine. Kawakita medical report 24: 315-318, 2009 (In Chinese).
6. Ji Q, Zhou J and Huang W: Immunohistochemical and in situ hybridization study of thyroid gonadotropin-releasing hormone receptor in rats. Chinese J Histochem Cytochem 11: 241-243, 2002 (In Chinese).
7. Emons G, Ortmann O, Becker M, Irmer G, Springer B, Laun R, Hölzel F, Schulz KD and Schally AV: High affinity binding and direct antiproliferative effects of LHRH analogues in human ovarian cancer cell lines. Cancer Res 53: 5439-5446, 1993.
8. Schottelius M, Berger S, Poethko T, Schwaiger M and Wester HJ: Development of novel ^{68}Ga- and ^{18}F-labeled GnRH-I analogues with high GnRHR-targeting efficiency. Bioconjug Chem 19: 1256-1268, 2008.
9. Mankoff DA, Link JM, Linden HM, Sundararajan L and Krohn KA: Tumor receptor imaging. J Nucl Med 49 (Suppl 2): 149S-163S, 2008.
10. Gründker C, Völker P and Emons G: Antiproliferative signaling of luteinizing hormone-releasing hormone in human endometrial and ovarian cancer cells through G protein alpha(I)-mediated activation of phosphotyrosine phosphatase. Endocrinology 142: 2369-2380, 2001.
11. Gerber B, von Minckwitz G, Stehle H, Reimer T, Felberbaum R, Maass N, Fischer D, Sommer HL, Conrad B, Ortmann O, *et al*: Effect of luteinizing hormone-releasing hormone agonist on ovarian function after modern adjuvant breast cancer chemotherapy: the GBG 37 ZORO study. J Clin Oncol 29: 2334-2341, 2011.
12. Emons G, Schröder B, Ortmann O, Westphalen S, Schulz KD and Schally AV: High affinity binding and direct antiproliferative effects of luteinizing hormone-releasing hormone analogs in human endometrial cancer cell lines. J Clin Endocrinol Metab 77: 1458-1464, 1993.
13. Moreau JP, Delavault P and Blumberg J: Luteinizing hormone-releasing hormone agonists in the treatment of prostate cancer: a review of their discovery, development, and place in therapy. Clin Ther 28: 1485-1508, 2006.

14. Rose A, Froment P, Perrot V, Quon MJ, LeRoith D and Dupont J: The luteinizing hormone-releasing hormone inhibits the anti-apoptotic activity of insulin-like growth factor-1 in pituitary alphaT3 cells by protein kinase C alpha-mediated negative regulation of Akt. J Biol Chem 279: 52500-52516, 2004.
15. Szende B, Srkalovic G, Schally AV, Lapis K and Groot K: Inhibitory effects of analogs of luteinizing hormone-releasing hormone and somatostatin on pancreatic cancers in hamsters. Events that accompany tumor regression. Cancer 65: 2279-2290, 1990.
16. Greco F and Vicent MJ: Combination therapy: opportunities and challenges for polymer-drug conjugates as anticancer nanomedicines. Adv Drug Deliv Rev 61: 1203-1213, 2009.
17. Duncan R: Polymer conjugates as anticancer nanomedicines. Nat Rev Cancer 6: 688-701, 2006.
18. Eidne KA, Flanagan CA, Harris NS and Millar RP: Gonadotropin-releasing hormone (GnRH)-binding sites in human breast cancer cell lines and inhibitory effects of GnRH antagonists. J Clin Endocrinol Metab 64: 425-432, 1987.
19. Barda Y, Cohen N, Lev V, Ben-Aroya N, Koch Y, Mishani E, Fridkin M and Gilon C: Backbone metal cyclization: novel ^{99m}Tc labeled GnRH analog as potential SPECT molecular imaging agent in cancer. Nucl Med Biol 31: 921-933, 2004.
20. Seitz S, Buchholz S, Schally AV, Weber F, Klinkhammer-Schalke M, Inwald EC, Perez R, Rick FG, Szalontay L, Hohla F, *et al*: Triple negative breast cancers express receptors for LHRH and are potential therapeutic targets for cytotoxic LHRH-analogs, AEZS 108 and AEZS 125. BMC Cancer 14: 847, 2014.
21. Rusiecki JA, Holford TR, Zahm SH and Zheng T: Breast cancer risk factors according to joint estrogen receptor and progesterone receptor status. Cancer Detect Prev 29: 419-426, 2005.
22. Van Den Bossche B and Van de Wiele C: Receptor imaging in oncology by means of nuclear medicine: current status. J Clin Oncol 22: 3593-3607, 2004.
23. Imai A, Takagi A, Horibe S, Takagi H and Tamaya T: Fas and Fas ligand system may mediate antiproliferative activity of gonadotropin-releasing hormone receptor in endometrial cancer cells. Int J Oncol 13: 97-100, 1998.
24. Cai W and Chen X: Multimodality imaging of vascular endothelial growth factor and vascular endothelial growth factor receptor expression. Front Biosci 12: 4267-4279, 2007.
25. Virgolini I, Traub T, Novotny C, Leimer M, Füger B, Li SR, Patri P, Pangerl T, Angelberger P, Raderer M, *et al:* Experience with indium-111 and yttrium-90-labeled somatostatin analogs. Curs Pharm Des 8: 1781-1807, 2002.
26. Meko JB, Doherty GM, Siegel BA and Norton JA: Evaluation of somatostatin-receptor scintigraphy for detecting neuroendocrine tumors. Surgery 120: 975-983, 1996.
27. Katsuno M, Adachi H, Doyu M, Minamiyama M, Sang C, Kobayashi Y, Inukai A and Sobue G: Leuprorelin rescues polyglutamine-dependent phenotypes in a transgenic mouse model of spinal and bulbar muscular atrophy. Nat Med 9: 768-773, 2003.
28. Reisinger I, Bohuslavitzki KH, Brenner W, Braune S, Dittrich I, Geide A, Kettner B, Otto HJ, Schmidt S and Munz DL: Somatostatin receptor scintigraphy in small-cell lung cancer: results of a multicenter study. J Nucl Med 39: 224-227, 1998.
29. Thakur ML, Marcus CS, Saeed S, Pallela V, Minami C, Diggles L, Le Pham H, Ahdoot R and Kalinowski EA. ^{99m}Tc-labeled vasoactive intestinal peptide analog for rapid localization of tumors in humans. J Nucl Med 41: 107-110, 2000.
30. Fekete M, Zalatnai A, Comaru-Schally AM and Schally AV: Membrane receptors for peptides in experimental and human pancreatic cancers. Pancreas 4: 521-528, 1989.
31. Szepeshazi K, Schally AV, Groot K and Halmos G: Effect of bombesin, gastrin-releasing peptide (GRP)(14-27) and bombesin/GRP receptor antagonist RC-3095 on growth of nitrosamine-induced pancreatic cancers in hamsters. Int J Cancer 54: 282-289, 1993.
32. Peremans K, Cornelissen B, Van Den Bossche B, Audenaert K and Van de Wiele C: A review of small animal imaging planar and pinhole spect Gamma camera imaging. Vet Radiol Ultrasound 46: 162-170, 2005.
33. Friess H, Berberat P, Schilling M, Kunz J, Korc M and Büchler MW: Pancreatic cancer: the potential clinical relevance of alterations in growth factors and their receptors. J Mol Med (Berl) 74: 35-42, 1996.
34. Schottelius M, Berger S, Poethko T, Schwaiger M and Wester HJ: Development of novel ^{68}Ga- and ^{18}F-labeled GnRH-I analogues with high GnRHR-targeting efficiency. Bioconjug Chem 19: 1256-1268, 2008.
35. Reubi JC and Maecke HR: Peptide-based probes for cancer imaging. J Nucl Med 49: 1735-1738, 2008.
36. Medina RA and Owen GI: Glucose transporters: expression, regulation and cancer. Biol Res 35: 9-26, 2002.
37. Wang R: Clinical outlook for radio-immunity imaging. Int J Radiat Med Nucl Med Volume 13: 40-42, 1989.
38. Wang R, Zhang C, Yu L and Guo Y: Clinical application of radioimmunoimaging with ^{99m}Tc-BDI-1 in the diagnosis of bladder cancer. Chin Med J (Engl) 113: 396-399, 2000.
39. Vriesendorp HM and Vriesendorp FJ: A review of the intravenous administration of radiolabeled immunoglobulin G to cancer patients. High or low protein dose? Cancer Biother Radiopharm l8: 35-46, 2003.
40. Kang JH and Chung JK: Molecular-genetic imaging based on reporter gene expression. J Nucl Med 49 (Suppl 2): 164S-179S, 2008.
41. Cai W and Chen X: Multimodality molecular imaging of tumor angiogenesis. J Nucl Med 49 (Suppl 2): 113S-128S, 2008.
42. de Jong M, Breeman WA, Bernard BF, Bakker WH, Schaar M, van Gameren A, Bugaj JE, Erion J, Schmidt M, Srinivasan A, *et a1*: [^{177}Lu-DOTA^{0},Tyr^{3}]octreotate for somatostatin receptor-targeted radionuclide therapy. Int J Cancer 92: 628-633, 2001.
43. Khan TS, Sundin A, Juhlin C, Långström B, Bergström M and Eriksson B: ^{11}C-metomidate PET imaging of adrenocortical cancer. Eur J Nucl Med Mol Imaging 30: 403-410, 2003.
44. Dietz DW, Dehdashti F, Grigsby PW, Malyapa RS, Myerson RJ, Picus J, Ritter J, Lewis JS, Welch MJ and Siegel BA: Tumor hypoxia detected by positron emission tomography with ^{60}Cu-ATSM as a predictor of response and survival in patients undergoing neoadjuvant chemoradiotherapy for rectal carcinoma: a pilot study. Dis Colon Rectum 51: 1641-1648, 2008.
45. Chao KS, Bosch WR, Mutic S, Lewis JS, Dehdashti F, Mintun MA, Dempsey JF, Perez CA, Purdy JA and Welch MJ: A novel approach to overcome hypoxic tumor resistance: Cu-ATSM-guided intensity-modulated radiation therapy. Int J Radiat Oncol Biol Phys 49: 117l-1182, 2001.
46. Dehdashti F, Grigsby PW, Mintun MA, Lewis JS, Siegel BA and Welch MJ: Assessing tumor hypoxia in cervical cancer by positron emission tomography with ^{60}Cu-ATSM: relationship to therapeutic response-a preliminary report. Int J Radiat Oncol Biol Phys 55: 1233-1238, 2003.
47. Suzuki T, Nakamura K, Kawase T and Kubo A: Monitoring of response to radiation therapy for human tumor xenografts using ^{99m}Tc-HL91 (4,9-diaza-3,3,10,10-tetramethyldodecan-2,11-dione dioxime). Ann Nucl Med 17: 131-138, 2003.
48. Mochizuki T, Kuge Y, Zhao S, Tsukamoto E, Hosokawa M, Strauss HW, Blankenberg FG, Tait JF and Tamaki N: Detection of apoptotic tumor response in vivo after a single dose of chemotherapy with ^{99m}Tc-Annexin V. J Nucl Med 44: 92-97, 2003.